Biomaterials 231 (2020) 119672

Contents lists available at ScienceDirect

Biomaterials

journal homepage: www.elsevier.com/locate/biomaterials

A self-doping conductive polymer hydrogel that can restore electrical impulse propagation at myocardial infarct to prevent cardiac arrhythmia and preserve ventricular function

Chongyu Zhang[a,b,1], Meng-Hsuan Hsieh[c,1], Song-Yi Wu[c], Shu-Hong Li[b], Jun Wu[b], Shi-Ming Liu[a], Hao-Ji Wei[d], Richard D. Weisel[b,e], Hsing-Wen Sung[c,**], Ren-Ke Li[b,e,*]

[a] Department of Cardiology, Second Affiliated Hospital of Guangzhou Medical University, Guangzhou, China
[b] Toronto General Hospital Research Institute, Division of Cardiovascular Surgery, University Health Network, Toronto, Canada
[c] Department of Chemical Engineering and Frontier Research Center on Fundamental and Applied Sciences of Matters, National Tsing Hua University, Hsinchu, Taiwan, ROC
[d] Division of Cardiovascular Surgery, Veterans General Hospital-Taichung, And College of Medicine, National Yang-Ming University, Taipei, Taiwan, ROC
[e] Division of Cardiac Surgery, Department of Surgery, University of Toronto, Toronto, Canada

ARTICLE INFO

Keywords:
Self-doping
Conductive polymer
Electrical impulse propagation
Myocardial infarction
Cardiac arrhythmia

ABSTRACT

Following myocardial infarction (MI), necrotic cardiomyocytes (CMs) are replaced by fibroblasts and collagen tissue, causing abnormal electrical signal propagation, desynchronizing cardiac contraction, resulting in cardiac arrhythmia. In this work, a conductive polymer, poly-3-amino-4-methoxybenzoic acid (PAMB), is synthesized and grafted onto non-conductive gelatin. The as-synthesized PAMB-G copolymer is self-doped in physiological pH environments, making it an electrically active material in biological tissues. This copolymer is cross-linked by carbodiimide to form an injectable conductive hydrogel (PAMB-G hydrogel). The un-grafted gelatin hydrogel is prepared in a similar manner as a control. Both test hydrogels not only provide an optimal matrix for CM adhesion and growth but also maintain CM morphology and functional proteins. The conductivity of PAMB-G hydrogel is *ca.* 12 times higher than that of gelatin hydrogel. Microelectrode array analyses reveal that a heart placed on the PAMB-G hydrogel has a higher field potential amplitude than that placed on the gelatin hydrogel and can pass current from one heart to excite another heart at a distance. The injection of PAMB-G hydrogel into the scar zone following an MI in a rat heart improves electrical impulse propagation over that in a heart that has been treated with gelatin hydrogel, and synchronizes heart contraction, leading to preservation of the ventricular function and reduction of cardiac arrhythmia, demonstrating its potential for use in treating MI.

1. Introduction

Following myocardial infarction (MI), sustained ischemia may cause the necrosis of cardiomyocytes (CMs) and the formation of fibrotic tissue in damaged areas, stimulating subsequent ventricular remodeling [1]. The nonconductive nature of fibrotic tissues contributes to electrical uncoupling of viable CMs in the infarcted region, producing a proarrhythmic heterogeneous milieu [2]. The lack of electrical connection between the healthy myocardium and islands of intact CMs in fibrotic matrices supports asynchronous ventricular contraction, resulting in progressive functional decompensation [3]. Electrically reconnecting isolated CMs with uninjured tissues by restoring impulse propagation across the infarct scar can resynchronize contraction and prevent adverse remodeling and ventricular dysfunction.

An injectable conductive polymer hydrogel may have potential for restoring electrical signaling propagation through the infarct region. Conductive polymers are appealing because they exhibit the electrical properties of semiconductors but with ease of processing and modifiable conductivity [4]. Biological applications of conductive polymers include transmitting electrical impulses in neurite cultures [5], regenerating nerves [6], repairing muscle [7,8], and healing wounds [9–11]. Most cardiac applications involve producing three-dimensional

* Corresponding author. Division of Cardiovascular Surgery, Toronto General Hospital Research Institute, University Health Network, 101 College Street, Toronto, Ontario, M5G 1L7, Canada.
** Corresponding author.
E-mail addresses: hwsung@mx.nthu.edu.tw (H.-W. Sung), renkeli@uhnresearch.ca (R.-K. Li).
[1] The first two authors (C.Y. Zhang and M.H. Hsieh) contributed equally to this work.

https://doi.org/10.1016/j.biomaterials.2019.119672
Received 1 October 2019; Received in revised form 29 November 2019; Accepted 4 December 2019
Available online 09 December 2019
0142-9612/

cardiac anisotropy for cardiac tissue engineering [12,13].

The use of bioconductive materials such as carbon nanotubes and silver nanowires to restore impulse propagation in an injured myocardium has been suggested, but not fully tested [14,15]. The biological applications of several conductive polymers, such as polyaniline, polypyrrole, and poly-3,4-ethylenedioxythiophene (PEDOT), have been investigated [16–18]. Doping is an essential step in the generation of a conductive polymer, during which a dopant that can remove or add an electron is incorporated [19]. However, doping is generally environmentally controlled. For example, polyaniline can be doped to become conductive only in an acidic solution; when pH exceeds 4.0 (in physiological pH environments), the polymer is non-conductive [20], limiting its usefulness in clinical applications.

In the current study, poly-3-amino-4-methoxybenzoic acid (PAMB), which is a carboxyl group-functionalized polyaniline [21], is utilized as a conductive polymer. The unique character of this polymer is its self-doping capacity at physiological pH values, maintaining its conductivity in biological tissues. To enhance its biocompatibility, PAMB was grafted onto gelatin (PAMB-G) and the copolymer was then crosslinked with carbodiimide, forming an injectable conductive polymeric hydrogel (PAMB-G hydrogel, Fig. 1). Gelatin is the hydrolyzed form of collagen, which is a critical component of the extracellular matrix, and so more closely mimics native tissues [22].

The as-prepared PAMB-G hydrogel is injected into the myocardial scar tissue one week after MI in a rat model. The electrical impulse propagation across the scarred tissue and its efficacy in reducing cardiac arrhythmia and preserving ventricular function are evaluated. The self-doping of PAMB, which is lacking in other conductive biomaterials, may ensure continued conductivity when PAMB is inserted into the infarcted heart, and the biocompatibility of gelatin may induce a less inflammatory response.

2. Materials and methods

2.1. Synthesis and characterization of PAMB-G copolymer

PAMB-G copolymer was synthesized with a 1:10 wt ratio of 3-amino-4-methoxybenzoic acid (AMB):gelatin, which was found in a preliminary study to have the highest conductivity, using an oxidative polymerization method [23]. Briefly, an aqueous 40% gelatin solution was firstly prepared by dissolving the required amount of gelatin powder (Sigma Aldrich, St Louis, MO, USA) in deionized (DI) water. Two hundred mg of AMB (Alfa Aesar, Ottawa, Canada) was then added to the solution, which was mechanically stirred. Oxidative polymerization was carried out by adding 273 mg ammonium persulfate [APS, $(NH_4)_2S_2O_8$] as a catalyst to polymerize AMB monomers and graft them onto the backbone of gelatin. After 24 h, the resulting PAMB-G copolymer was dialyzed in DI water and freeze-dried for at least two days.

Fourier-transform infrared spectroscopy (FT–IR, Thermo Scientific, Nicolet iS50, Madison, WI, USA) and proton nuclear magnetic resonance (^{1}H NMR, Bruker Avance-500 spectrometer, Rheinstein, Germany) were used to assess the conjugation of PAMB on gelatin. FT–IR spectra of freeze-dried samples were acquired and ^{1}H NMR spectra of test samples in DMSO-d_6, to which a few drops of hydrochloric acid (HCl) had been added, were also obtained. The amount of PAMB that had been grafted on the PAMB-G copolymer was determined from UV–vis spectra (SpectraMax M5 Microplate Reader, Molecular Devices, Sunnyvale, CA, USA) [24]. The self-doping characteristics of the as-synthesized PAMB-G copolymer at various pH values were determined from their UV–vis optical properties, which were measured using the SpectraMax M5 Microplate Reader.

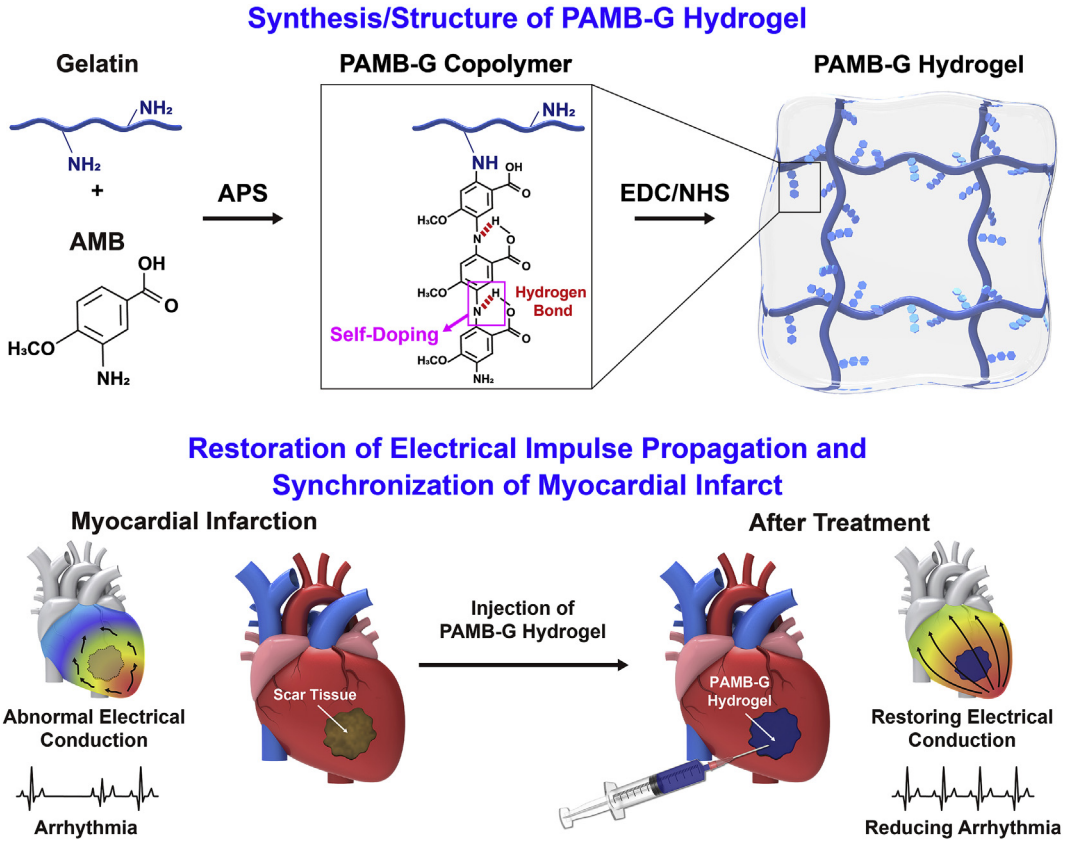

Fig. 1. Synthesis and structure of PAMB hydrogel and mechanism of its restoring electrical impulse propagation and synchronizing myocardial contraction following a myocardial infarction.

2.2. Formation and characterization of PAMB-G hydrogel

The formation of the conductive hydrogel was induced by the addition of 1-ethyl-3-(3-dimethylaminopropyl) carbodiimide hydrochloride (EDC, 48 mM, Themo Scientific, Rockford, IL, USA) as a crosslinker to the PAMB copolymer in the presence of *N*-hydroxysuccinimide (NHS, 24 mM, Sigma Aldrich). The gelatin hydrogel, which was used as a control in the study, was prepared in the same way except for the addition of AMB. EDC is a non-toxic crosslinking agent [25].

The rheological behaviors of gelatin and PAMB-G hydrogels were revealed at 37 °C by analyzing their storage (G′) and loss (G″) moduli as a function of reaction time and angular frequency [26]. A compression test was performed on gelatin and PAMB-G hydrogels using an Instron material testing instrument (Mini 44, Canton, MA, USA) at a constant speed of 5 mm/min, and the Young's modulus was determined from the initial slope of the stress–strain curve in the elastic region.

The conductivity of gelatin and PAMB-G hydrogels was evaluated using a two-probe conductive analyzer (Hewlett-Packard Development Company, Palo Alto, CA, USA). Test hydrogels were placed on a platform, and two probes at 7 mm from each other were used for conductivity measurements in linear double-sweep mode.

2.3. Animal studies

Sprague–Dawley (SD) rats (neonatal or adult weighing 225–250 g) were obtained from Charles River Laboratories (Saint-Constant, QC, Canada). All animal protocols and procedures were approved by the Animal Research Center of the University Health Network and followed the Guide for the Care and Use of Laboratory Animals (NIH, 8th Edition, 2011).

2.4. Cardiomyocyte isolation and cell compatibility analysis

CMs were isolated from neonatal SD rats using enzymatic dissociation methods as previously described [27]. Briefly, atria were removed from the hearts, and the ventricles were minced and digested with 0.15% trypsin (Life Technologies, Burlington, ON, Canada) at 37 °C. The isolated cells were pre-plated on a non-coated dish for 30 min to reduce contamination of the cardiac fibroblasts. The cells were plated at a density of $1.5 \times 10^5/cm^2$ in 1:1 DMEM:Ham F12 (Life Technologies) that contained 10% fetal bovine serum (FBS), 100 U/mL penicillin G, and 0.1 mg/mL streptomycin. BrdU (5-bromo-2′-deoxyuridine, 0.1 mM, Sigma Aldrich) was added to the cells to prevent the growth of non-myocytes in the early stages of the experiment. After the first day of culture, the BrdU was removed, and the cells were cultured in the same medium as above, but with 8% FBS.

To assess their cell compatibility, CMs were plated on uncoated polystyrene culture dishes (CDs) or on CDs that were coated with gelatin or PAMB-G hydrogel at a concentration of 1.5×10^6/35 mm dish. After three days, cells were fixed and examined by scanning electron microscopy (SEM). To measure cell proliferation, the plated CMs were trypsinized and counted using a hemocytometer with trypan blue exclusion assay after one, three, or five days in culture.

2.5. Identification of expression of cardiac functional proteins in CMs

Immunofluorescent staining was performed to identify the cardiac functional proteins sarcomeric α-actinin (SARC) and connexin 43 in CMs that were cultured on CDs or that had a coating of gelatin or PAMB-G hydrogel, for three days after seeding. Cultured cells were fixed in 2% paraformaldehyde for 10 min, blocked in 5% donkey serum, and then incubated with monoclonal anti-SARC (1:800; Abcam, AB9465) or rabbit anti-connexin 43 (1:800; Sigma Aldrich, C6219), followed by an Alexa546 donkey anti-mouse or rabbit IgG secondary antibody (1:400; Life Technologies). Nuclei were counterstained with 4′,6-diamidino-2-phenylindole (DAPI, Sigma Aldrich).

2.6. Evaluation of electrical conduction through PAMB-G hydrogel

An *ex vivo* model was constructed to determine whether electrical conduction occurred through the gelatin or PAMB-G hydrogel using a biological current that was generated by a Langendorff-perfused heart [28]. In the study, the hearts of SD rats were excised after the animals had been heparinized and euthanized by an isoflurane overdose (5%). To stop the heart and preserve cell viability during ischemia, retrograde perfusion was performed with an ice-cold cardioplegic solution (140 mM NaCl, 4 mM Tris, 30 mM KCl, 5 mM $MgSO_4$, 25 mM glucose, 30 mM histidine, pH 7.15). The heart was then cannulated using a blunted 27G needle that was inserted into the aortic root and perfused with cardioplegic solution at a rate of 3 mL/min for 10 min. Finally, the cannulated heart was excised, placed on a customized Langendorff apparatus, perfused with the Krebs-Henseleit solution (117 mM NaCl, 24 mM $NaHCO_3$, 11.5 mM glucose, 3.3 mM KCl, 1.25 mM $CaCl_2$, 1.2 mM $MgSO_4$, 1.2 mM KH_2PO_4), and aerated with carbogen (5% CO_2/95% O_2) at 37 °C at a rate of 5 mL/min.

The established *ex vivo* model was used in a one-heart or two-heart system to evaluate the electrical conductivity of the test hydrogel. In the one-heart system, one heart that had been isolated from SD rats and perfused with a Langendorff apparatus was placed on top of the gelatin or PAMB-G hydrogel of various thicknesses (2.0, 4.0, and 6.0 mm). A 36-lead flexible microelectrode array (MEA) was placed on the bottom of the test hydrogel to measure local field potentials. In the two-heart system, one *ex vivo* Langendorff-perfused beating heart was placed on one side of the gelatin or PAMB-G hydrogel with a thickness of 1.0, 2.0, 3.0, or 4.0 mm. A second non-beating heart was placed on the other side of the gelatin or PAMB-G hydrogel. The non-beating heart had received a cardioplegic solution that contained 20 mEq of potassium chloride, rendering it non-beating. Electrocardiography (ECG, AD Instruments, Colorado Springs, CO, USA) was used to record any electrical activity from the non-beating heart.

2.7. In vitro and ex vivo imaging of calcium (Ca^{2+}) transient and electrical signal propagation

In vitro CM Ca^{2+} transient propagation was studied by incubating CMs with the Ca^{2+} indicator Fluo-4 AM (acetoxymethyl, 5 μM, F14217) in enhancing medium Pluronic® F-127 (P3000MP, both from Life Technologies) for 30 min. The incubated CMs were then washed with Tyrode's solution. Ca^{2+} transient propagation in CMs was assessed by the excitation of Fluo-4 AM at 488 nm, and emission at > 515 nm was detected.

Electrical impulse propagation through the left ventricle of the heart was optically mapped. The electrical signal conduction kinetics of the *ex vivo* Langendorff-perfused rat hearts was measured by perfusing the hearts for 10 min at a rate of 3 mL/min with 10 μM of the voltage-sensitive dye di-4-ANEPPS (Life Technologies) that was diluted in a high-potassium cardioplegia solution. Di-4-ANEPPS was excited at 510 nm, and emission at > 570 nm was detected.

Both Ca^{2+} transient propagation and electrical signal conduction kinetics were recorded using an optical high-speed electron multiplied charge coupled-device (EMCCD) camera system (Evolve 128, Photometrics, Tucson, AZ, USA) that was coupled to a dissecting microscope. Ca^{2+} transients were recorded at 485 frames/s with a resolution of 60.5 μm/pixel, while electrical impulse images were recorded at 883 frames/s with a resolution of 191.9 μm/pixel. To record the electrical signal from the Langendorff-perfused rat hearts, the scar tissue was positioned in the center of the view. The starting time for measurements was when the first electrical signal that appeared on the heart within the view and marked as time 0, and the marked end time was when the electrical signal had finished propagating (the time of the last frame before the electrical signal in healthy hearts had propagated out of the view). All data were obtained using μ-Manager (NIH) and analyzed using ImageJ and BV Analyze software (BrainVision,

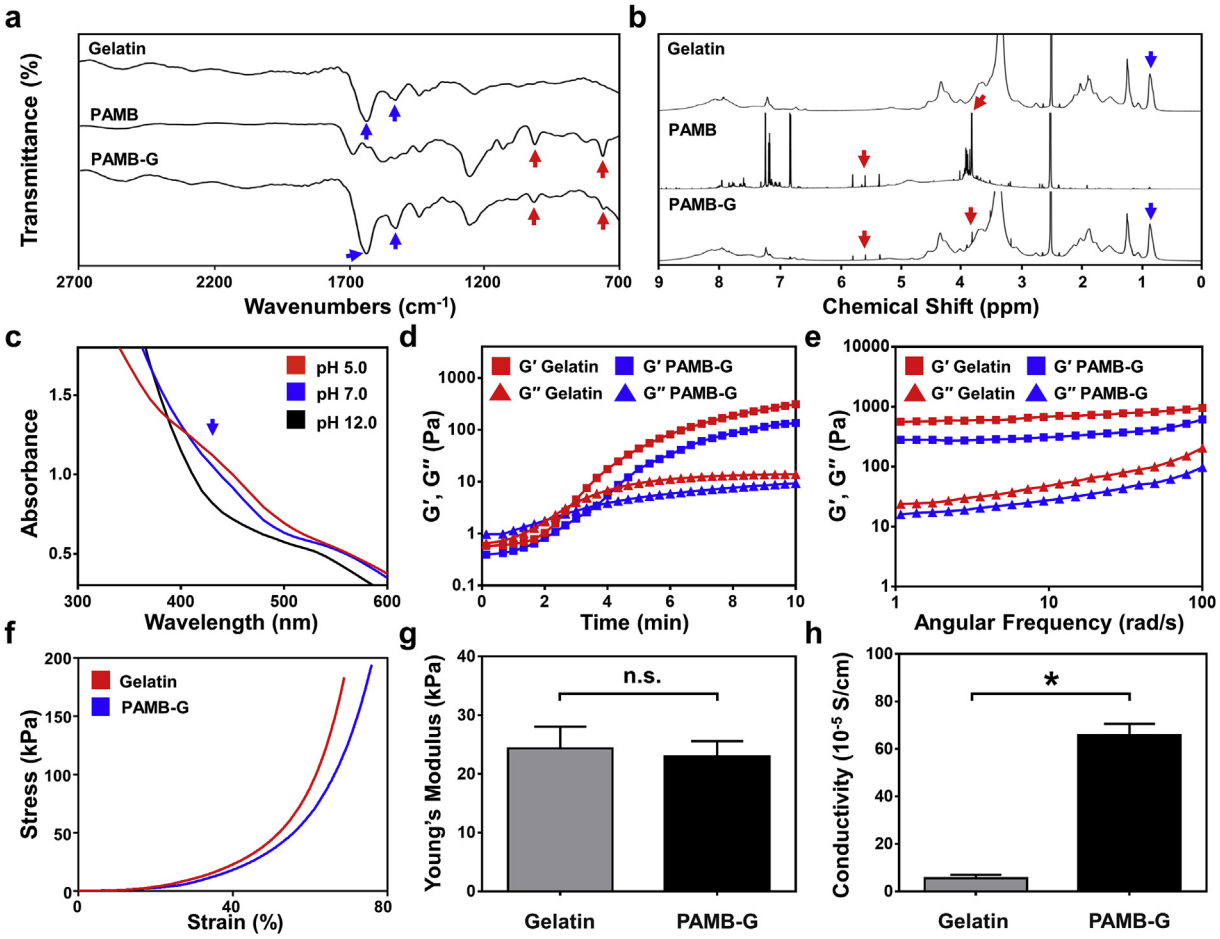

Fig. 2. (a) FT–IR and (b) ^{1}H NMR spectra of gelatin, PAMB, and PAMB-G copolymer, showing successful conjugation of PAMB on gelatin backbone. (c) UV–vis spectra of PAMB-G copolymer at various pH values, demonstrating its self-doping characteristics under physiological pH conditions. Rheological behaviors of gelatin and PAMB-G hydrogels in (d) time sweep and (e) frequency sweep mode. (f) Stress–strain curves and (g) Young's moduli of gelatin and PAMB-G hydrogels (n = 7 each group). (h) Conductivities of gelatin and PAMB-G hydrogels (n = 7 each group). *P < 0.05; n.s.: not significant.

Morrisville, NC). Parts of recordings that contained visible fluorescence were processed using a low-pass filter at 100 Hz and pseudocolored. Multiple processed images were stacked to generate isochronal maps of peak signal propagation over time.

2.8. Hydrogel injection and electrical activity analysis in an acute MI model

Adult female SD rats (200–250 g) were used in the study. Permanent ligation of the left descending coronary artery was performed to generate an animal model with MI. At one-week post infarction, echocardiography was performed to determine the infarct size and cardiac function. The size of the scar was approximately one third of the area of the anterior and apical region of the left ventricle. To minimize the variation of the animal model, only animals that exhibited 25–35% fractional shortening were included in the study.

Equal amounts of test hydrogel (25% by weight) were injected into each of the three injection sites (ca. 33 μL at each site, 100 μL in total) in the infarct area - one at the center of the scar, one half way between the center and the right border of the scar, and the third half way between the center and the left border of the scar. The hydrogels were injected into the middle layer of the myocardium, and covered the entire fibrotic infarct scar area, including the border zone. No animal died as a result of the injection procedure.

Regional field potential amplitudes on the fibrotic scar tissue that had formed at four weeks post-hydrogel injection were measured by a 36-lead flexible MEA, while global fibrotic scar tissue field potential amplitudes were evaluated by an 8-lead ECG catheter. Spontaneous premature ventricular contractions (PVCs) or ventricular tachycardia (VT) at four weeks post-hydrogel treatment was monitored by telemetry and calculated as the number of arrhythmias per hour.

Induced arrhythmia was assessed by programmed electrical stimulation (PES). Standard clinical PES protocols were employed, involving the applications of extra burst (120 ms cycle length), single (70 ms cycle length), double (60 ms cycle length), and triple (50 ms cycle length) stimuli under spontaneous rhythm. Susceptibility to arrhythmia was determined using an inducibility quotient as follows: hearts with no PVCs or VT received a score of 0; non-sustained PVCs or VT (≤15 beats) that was induced by three extra stimuli was given a score of 1; sustained PVCs or VT (> 15 beats) that was induced by three extra stimuli was given a score of 2; non-sustained PVCs or VT that was induced by two extra stimuli was given a score of 3; sustained PVCs or VT that was induced by two extra stimuli was given a score of 4; non-sustained PVCs or VT that was induced by one extra stimulus was given a score of 5; sustained PVCs or VT that was induced by one extra stimulus was given a score of 6; sustained or non-sustained PVCs or VT that was induced after the train of eight stimuli was given a score of 7; asystole after the termination of pacing was given a score of 8. A higher score indicated greater susceptibility to arrhythmia [29].

2.9. Cardiac function assessment and histological examination

Echocardiography (GE Vivid 7 Ultrasound System, GE Healthcare, Canada) was applied to both gelatin or PAMB-G groups to assess their cardiac functions with respect to their fractional shortening, ejection

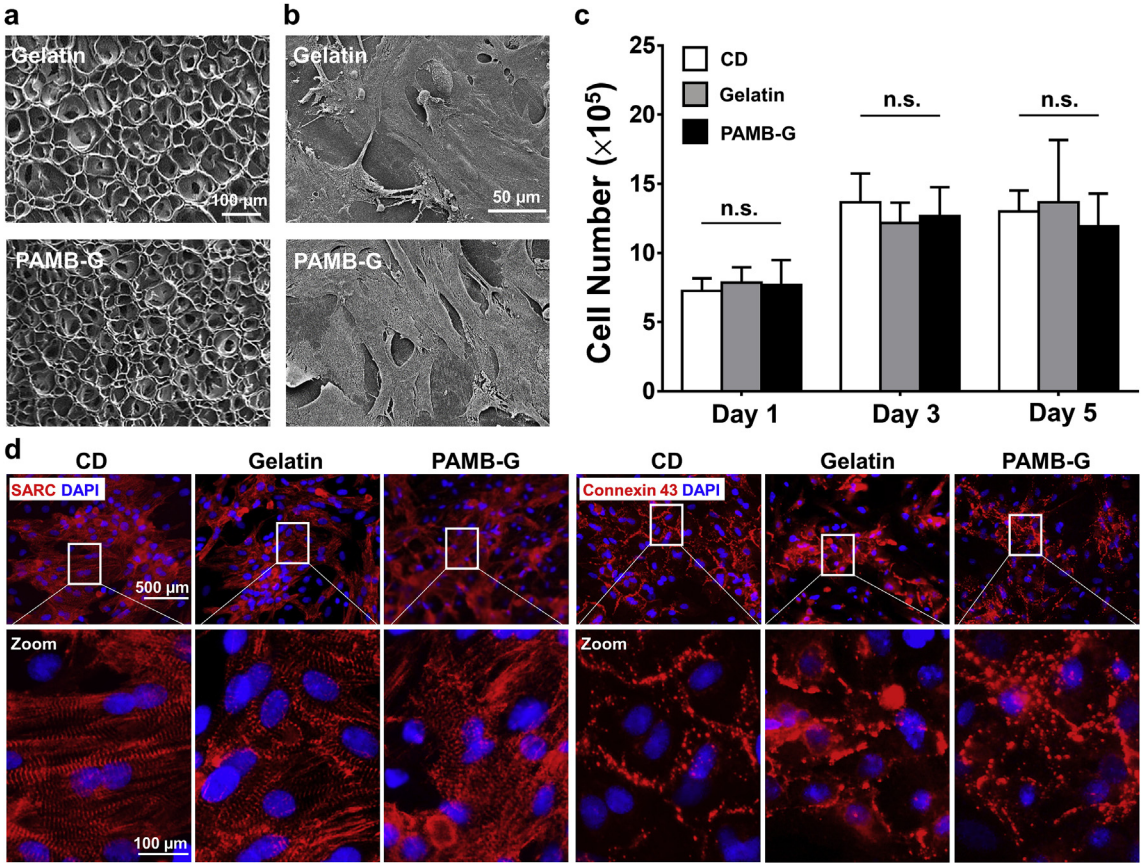

Fig. 3. (a) SEM micrographs of gelatin and PAMB-G hydrogels, showing their physical structures. (b) CMs grown on gelatin or PAMB-G hydrogel at day three following cell seeding, showing normal cell morphology. (c) Numbers of CMs grown on culture dish (CD) alone or with a coating of gelatin or PAMB-G hydrogel during five days in culture, showing that both gelatin and PAMB-G hydrogels supported CM growth (n = 3 each group). (d) Representative fluorescence photomicrographs of SARC and connexin 43 staining of CMs that were cultured on CD, or had a coating of gelatin or PAMB-G hydrogel, captured three days following seeding. n.s.: not significant.

fraction, and left ventricular internal systolic (LVIDs) and diastolic (LVIDd) dimensions [30]. Four weeks after the test hydrogel was injected, animals were sacrificed, and their hearts were retrieved, cut into slices, and grossly examined [31]. Tissue sections were stained with hematoxylin and eosin (H&E) or Masson's trichrome and their histological changes were thus observed. Immunofluorescent staining was also conducted to detect SARC and connexin 43 in the infarcted myocardium.

2.10. Statistical analysis

Data are expressed as mean ± SD. Analyses were performed using GraphPad Prism version 7.0 software (GraphPad software, San Diego, CA, USA). Student's *t*-test was used to make two-group comparisons. Comparisons of parameters among three or more groups were made using one-way analysis of variance (ANOVA) for single-factor variables followed by Tukey *post-hoc* tests or two-way ANOVA for two-factor variables with repeated measurements over time, followed by Bonferroni *post-hoc* tests. Differences were regarded as statistically significant at $P < 0.05$.

3. Results and discussion

Matrix biopolymers have the beneficial effect of preserving cardiac function after an MI by providing structural support to prevent thinning and dilation of the infarct scar [32–34]. However, non-conductive biomaterials, such as gelatin or collagen, when implanted into non-contractile fibrotic tissues, cannot reverse their delayed impulse propagation [35]. This work presents a self-doping conductive PAMB-G hydrogel that can be injected into scar tissues to improve electrical impulse propagation and electrically activate isolated contracting regions, improving preservation of ventricular function.

3.1. Characteristics of PAMB-G copolymer

To create an electrically conductive polymer, AMB monomers were polymerized and grafted onto non-conductive gelatin, forming PAMB-G copolymer. The FT-IR spectrum of PAMB-G copolymer in Fig. 2a includes two characteristic peaks at 1644 and 1533 cm^{-1}, corresponding to the amide I (C═O stretching vibration) and the amide II (N–H bending vibration) of gelatin, respectively. Peaks were also observed at 764 and 1022 cm^{-1}, and these were attributed to the characteristic aromatic C–H out-of-plane bending vibration and the C–O–C stretching vibration of PAMB, respectively. The ^{1}H NMR spectrum of PAMB-G copolymer exhibited signals in the range of 5.2–5.8 ppm and a signal at 3.8 ppm, which were associated with the protonated NH groups and the OCH_3 group on PAMB, and a signal at 0.8 ppm, which was attributed to the alkyl groups on gelatin (Fig. 2b). These analytical results verify that PAMB had been successfully grafted onto the gelatin backbone (PAMB-G copolymer). The amount of PAMB grafted on the PAMB-G copolymer was 7.3 ± 0.2% by weight, as determined by measuring its absorbance at 500 nm with a spectrophotometer (n = 6 batches).

To examine its variation in the electronic structure of PAMB copolymer in physiological pH environments, UV–vis spectra of aqueous PAMB-G copolymer at various pH values were recorded [36]. According to Fig. 2c, the spectra of PAMB-G at pH 5.0 and 7.0 included a

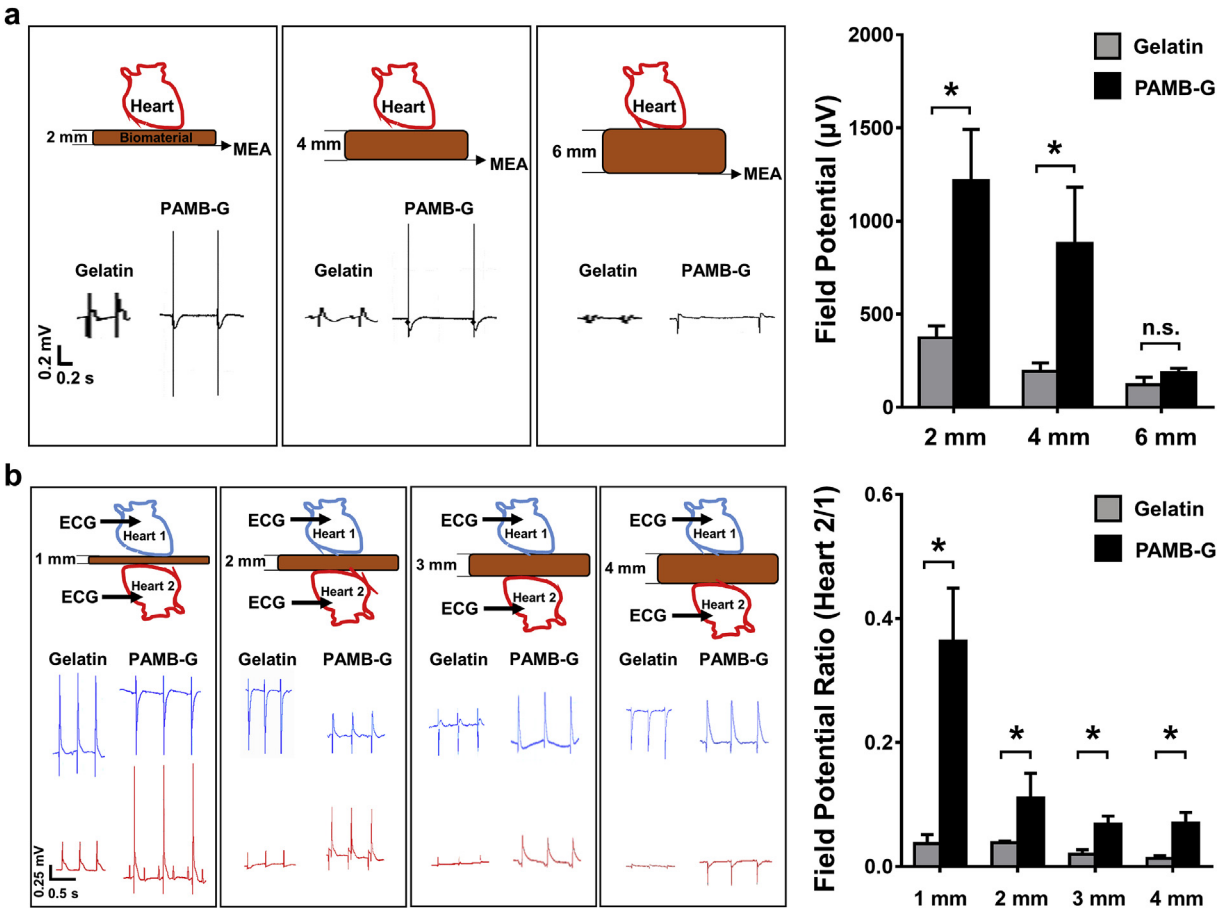

Fig. 4. (a) An *ex vivo* beating rat heart was placed on gelatin or PAMB-G hydrogel with a thickness of 2, 4, or 6 mm. Local field potential amplitudes that were detected through test hydrogels using a MEA (n = 4 each group). (b) Representative ECG recordings of stimulation signals from an *ex vivo* beating heart (Heart 1) that passed through gelatin or PAMB-G hydrogel with a thickness of 1, 2, 3, or 4 mm to a non-beating heart (Heart 2); local field potential ratios of non-beating hearts (Heart 2)/beating hearts (Heart 1) (n = 4 each group). *$P < 0.05$; n.s.: not significant.

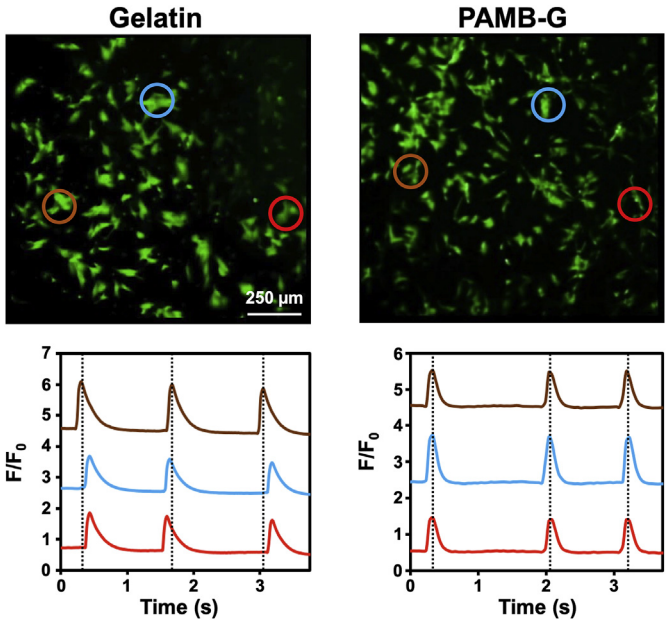

Fig. 5. Ca^{2+} transient propagation through distinct clusters of spontaneously beating CMs grown on gelatin or PAMB-G hydrogel at day three following cell seeding; CMs grown on PAMB-G hydrogel exhibit better synchronization than those grown on gelatin hydrogel.

broad absorption band at 420–440 nm as a result of a polaron transition, suggesting that the copolymer was highly conductive [21]. PAMB exhibits intra-molecular hydrogen bonding between the carboxyl group and the amine of the aniline in its repeating unit (Fig. 1). This hydrogen bonding reduces the electron density of the nitrogen, ultimately rendering the PAMB self-doped at pH values that exceeds 4.0. As it is a structural part of the polymeric backbone, the carboxyl dopant group does not leach away, favoring the stability of the doped copolymer, making the self-doped PAMB an electrically active material in a physiological pH environment. Furthermore, hydration may occur at the hydrogen-bonding sites of PAMB, increasing its solubility and, therefore, processability in aqueous solutions, favoring its clinical use. As the environmental pH was elevated to 12.0, the polaron band in the spectrum of PAMB-G was significantly suppressed, revealing a dedoping effect.

3.2. Characteristics of PAMB-G hydrogel

To form the PAMB-G hydrogel, the as-prepared PAMB-G copolymer was cross-linked by the addition of EDC and NHS. Gelatin hydrogel was prepared similarly, using plain gelatin molecules, as a control. The gelation behaviors of gelatin and PAMB-G hydrogels were individually characterized by analyzing their rheological properties. In reaction time sweep mode (Fig. 2d), the crossover points of the storage modulus G′ and loss modulus G″, corresponding to the durations of gelation [37], were detected within 5 min for both test samples. Such a gelation duration may provide sufficient working time for injection of the hydrogel, while preventing its premature gelation inside the syringe

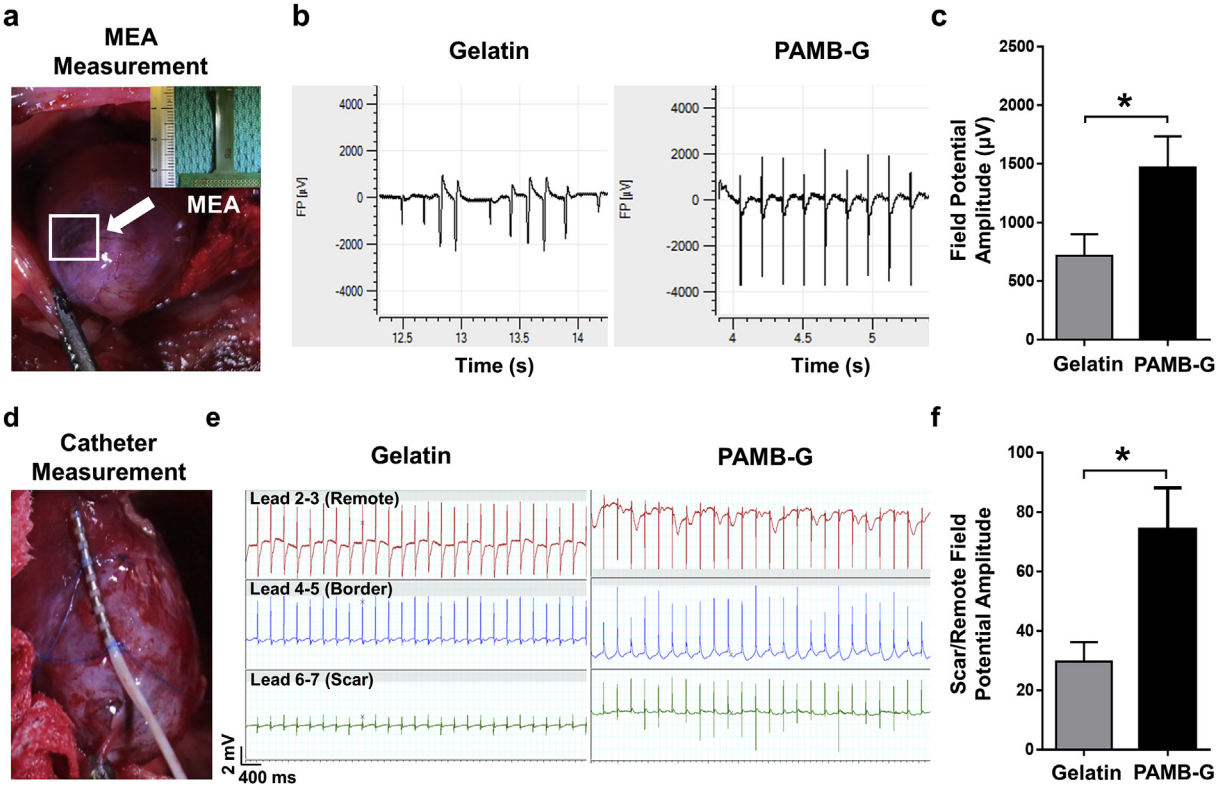

Fig. 6. (a) Regional field potential amplitude of fibrotic scar tissue at four weeks post-injection of gelatin or PAMB-G hydrogel, measured by a 36-lead flexible microelectrode array (MEA). (b) Representative electrograms and (c) regional field potential amplitudes measured in fibrotic scar tissues (n = 6 each group). (d) Global field potential amplitude across fibrotic scar tissue at four weeks post-injection of gelatin or PAMB-G hydrogel, measured by an 8-lead catheter. (e) Representative electrograms detected at remote, border, and scar areas and (f) ratios of scar/remote field potential amplitudes (n = 5 each group). *$P < 0.05$.

[38,39]. In angular frequency sweep mode (Fig. 2e), G′ dominated G″ over the entire frequency range, indicating that both test samples behaved like elastic solids [40].

The Young's moduli that were obtained from the stress–strain curves (Fig. 2f and g) demonstrate that both gelatin and PAMB-G hydrogels had similar compression elasticities, which were close to that of the native myocardium (11.9–46.2 kPa [41]), suggesting that both hydrogels were suitable for use as a biomaterial in beating hearts. As measured by a two-point probe, the conductivity of PAMB-G hydrogel was *ca*. 12 times higher than that of gelatin hydrogel (Fig. 2h). These findings suggest the successful conjugation and formation of an electrically conductive polymeric hydrogel.

3.3. Physical structure of PAMB-G hydrogel and its cell compatibility

The physical structures of gelatin and PAMB-G hydrogels were separately examined by SEM. As shown in Fig. 3a, both gelatin and PAMB-G hydrogels showed similar, well-structured gel networks, indicating that the conjugation of PAMB did not alter the physical structure of the gelatin hydrogel. Gelatin is a necessary component of extracellular matrices and has a wide range of uses in support of cell adhesion and growth [42]. Therefore, gelatin was chosen as the structural backbone to which PAMB was grafted, yielding a conductive biomaterial with superior biocompatibility.

The effects of PAMB-G hydrogel on the survival of CMs were assessed to see whether adding PAMB to gelatin hydrogel was toxic to cells. Neonatal rat CMs were grown on plates that were coated with gelatin hydrogel or PAMB-G hydrogel, or they were grown directly on CDs as a normal control. As shown in Fig. 3b and S1, CMs grown on the gelatin or PAMB-G hydrogel showed normal cell morphology. Quantification of CMs that were seeded at the same initial seeding density on CDs alone as with a coating of gelatin or PAMB-G hydrogel through trypsinization and cell counting demonstrate that both gelatin and PAMB-G hydrogels supported CM growth to a similar degree to that provided by CDs (Fig. 3c).

The subcellular proteins that are important for normal CM function were analyzed in detail. Immunofluoresent staining was used to detect SARC and connexin 43 in CMs that were cultured on CDs or those with a coating of gelatin or PAMB-G hydrogel. The CMs in all three groups exhibited a typical lattice structure that was interconnected by rod-shaped α-actinin with punctuate gap junction protein connexin 43 mostly around the plasma membrane (Fig. 3d). Taken together, these data support the hypothesis that the gelatin-based bioconductive material (PAMB-G hydrogel) not only functioned as the optimal matrix for CM adhesion and growth but also maintained CM morphology and functional proteins.

3.4. Electrical conduction through PAMB-G hydrogel

An ideal cardiac conductive biomaterial must be able to restore electrical conduction (or electrical impulse propagation) across the scarred tissue. To ascertain the capacity of PAMB-G hydrogel to support conduction between tissues at a distance, an *ex vivo* model was used to determine whether electrical impulse propagation could occur through the test hydrogel using biological current that was generated by a Langendorff-perfused heart. MEA measurements in a one-heart system indicate that the local field potential amplitude that was measured through the PAMB-G hydrogel significantly exceeded that through the gelatin hydrogel with the tested thicknesses indicated ($P < 0.05$, Fig. 4a). In the two-heart system, the field potential amplitude that was detected on the non-beating heart that was placed on the other side of PAMB-G hydrogel significantly exceeded that of the heart that was placed on the gelatin hydrogel over the entire range of investigated thicknesses ($P < 0.05$, Fig. 4b). The above data establish that the

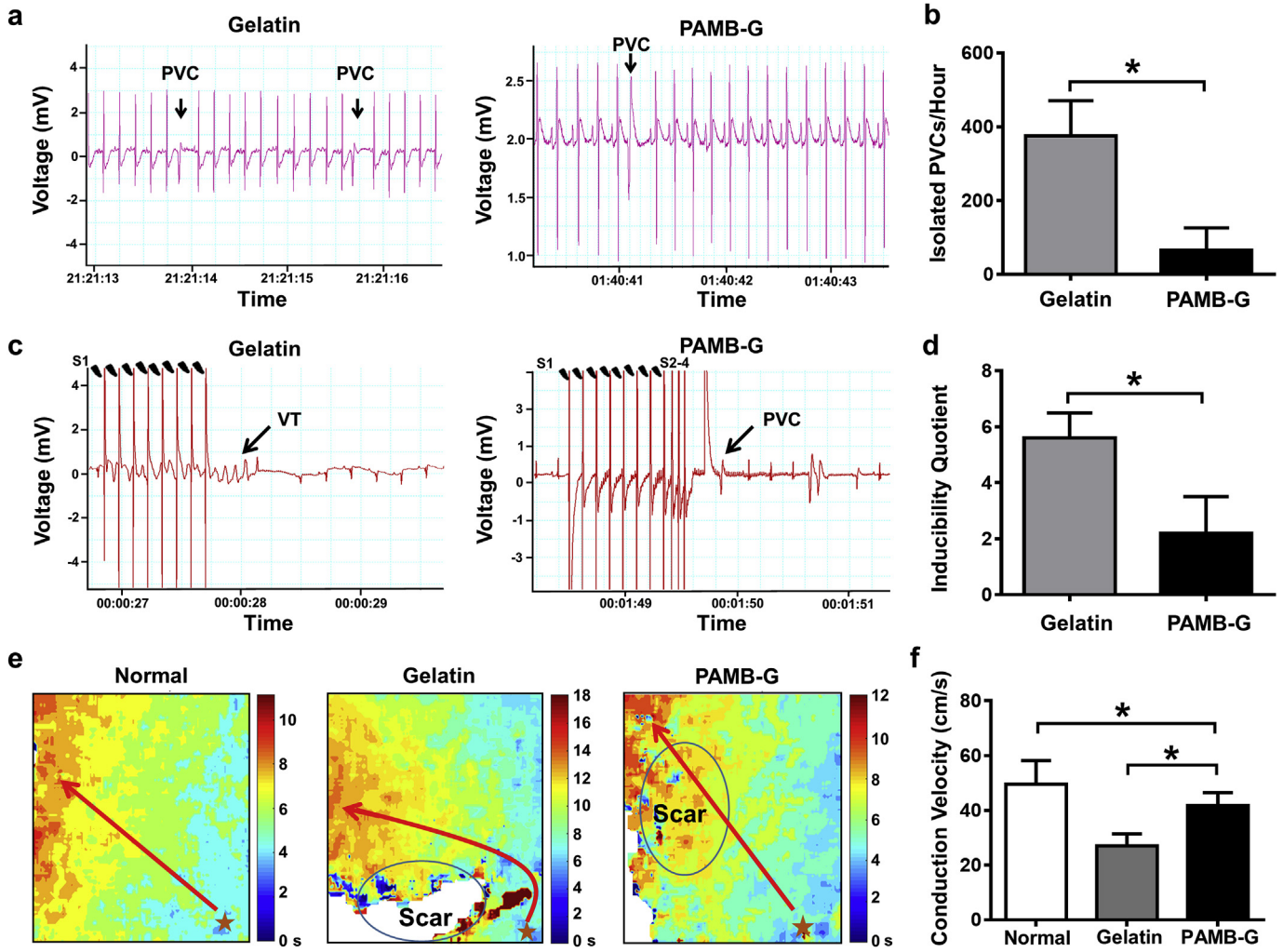

Fig. 7. (a) Electrograms of spontaneous arrhythmias recorded by ambulatory telemetry at four weeks post-injection of test hydrogel, showing that (b) PAMB-G group had a lower rate of spontaneous PVCs than gelatin group (n = 5 each group). (c) Electrograms of induced arrhythmias recorded at four weeks post-hydrogel injection after programmed electrical stimulation (PES), showing that (d) PAMB-G group had a lower induced inducibility quotient than gelatin group (n = 5 each group). (e) Optical mappings of electrical impulse propagation (red arrows) through left ventricles of normal heart or of heart treated with gelatin or PAMB-G hydrogel, indicating (f) that PAMB-G-treated hearts had a significantly higher conduction velocity than gelatin-treated hearts (n = 6 each group). *$P < 0.05$. (For interpretation of the references to color in this figure legend, the reader is referred to the Web version of this article.)

PAMB-G hydrogel supported electrical conduction between tissues at a distance, implying its potential ability to restore electrical impulse propagation across scarred tissue in an *in vivo* setting.

3.5. Ca^{2+} transient propagation through distinct CM clusters

To investigate whether PAMB-G hydrogel promotes electrical conduction at the cellular level, spontaneously beating CMs that were isolated from neonatal rats were grown in clusters on dishes that were coated with gelatin or the PAMB-G hydrogel. Cytoplasmic Ca^{2+} transient propagation through distinct CM clusters was measured as an indirect indicator of action potential propagation [43]. According to Fig. 5 and Movie S1, the Ca^{2+} transient of distinct clusters of spontaneously beating CMs that were grown on the PAMB-G hydrogel had better synchronization than that of CMs that were grown on the gelatin hydrogel. These results indicate that PAMB-G hydrogel promoted electrical conduction and established the synchronization of distinct clusters of beating CMs without the application of an external electrical impulse.

Supplementary data related to this article can be found at https://doi.org/10.1016/j.biomaterials.2019.119672.

3.6. Regional and global electrical field potential amplitudes in scar tissues

Encouraged by the above *in vitro* and *ex vivo* conduction results, the effects of test hydrogels on the electrical activity of cardiac scar tissues *in vivo* were evaluated using a rat MI model. The test hydrogel was injected directly into the scar tissue, which covered the entire scar area (Fig. 1). Four weeks post-hydrogel injection, a flexible MEA was used to measure the regional electrical field potential across the scar area (Fig. 6a). As indicted in Fig. 6b and c, the regional electrical field potential amplitude around the scar area was significantly higher in the PAMB-G-injected hearts than in the gelatin-injected hearts ($P < 0.05$). The global cardiac surface field potential amplitude at four weeks post-hydrogel injection was measured using an 8-lead catheter (Fig. 6d). Fig. 6e and f indicate that the PAMB-G-injected hearts had a higher scar/remote field potential amplitude ratio than did the gelatin-injected hearts ($P < 0.05$). These experimental results suggest that PAMB-G hydrogel injection improves electrical activity in fibrotic tissues and facilitates electrical current propagation across the scar region.

3.7. Spontaneous and induced arrhythmias in infarcted hearts

Myocardial scar tissue is composed of fibrillary cross-linked

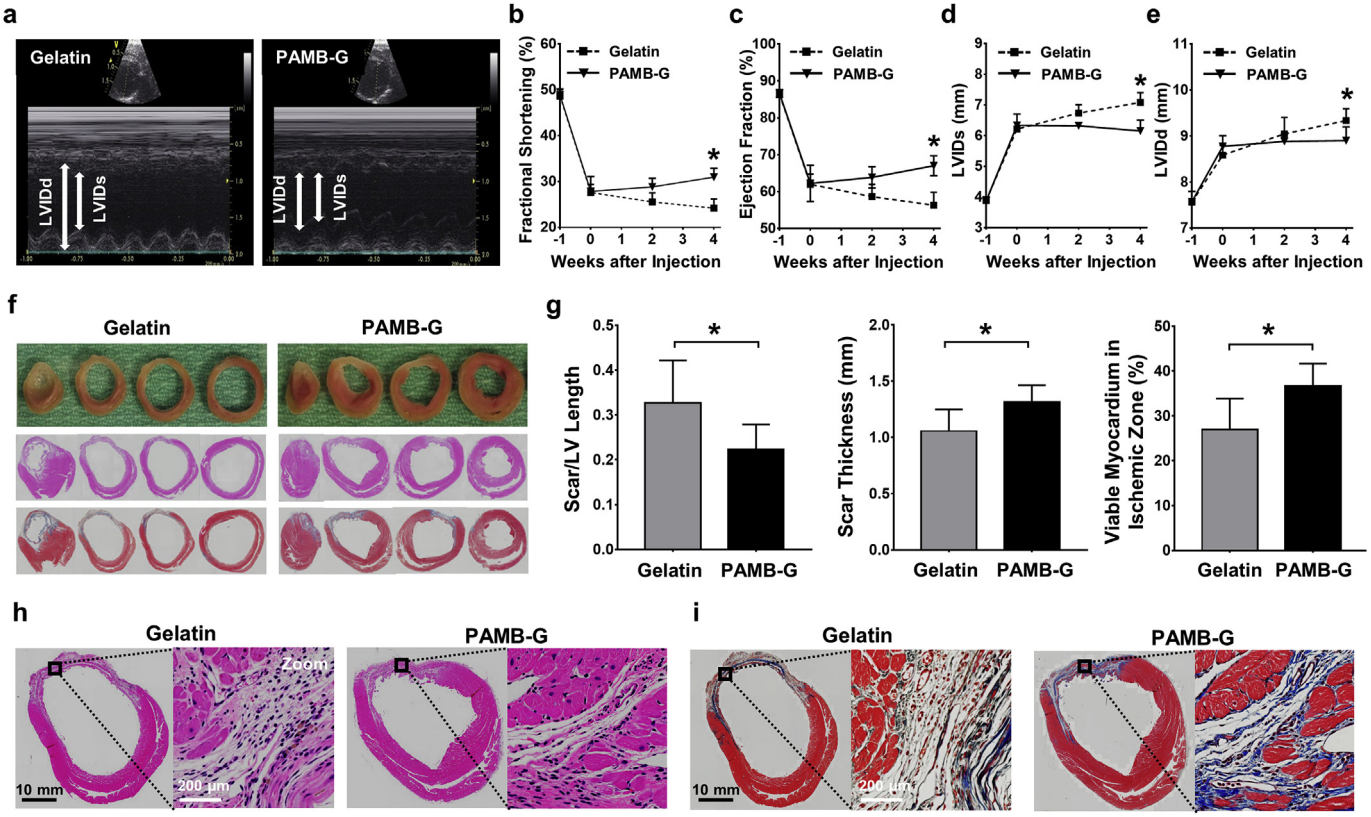

Fig. 8. (a) Representative M-mode echo images obtained four weeks following test hydrogel injection, showing that PAMB-G group had greater (b) fractional shortening and (c) ejection fraction with smaller (d) LVIDs and (e) LVIDd than gelatin group. (f) Representative photographs of whole sectioned hearts at four weeks following test hydrogel injection, showing that (g) scars were smaller and scar thickness and viable myocardium were greater in PAMB-G group than in gelatin group. Photomicrographs of (h) H&E and (i) Masson's trichrome staining. (b–e, n = 8 each group; f and g, n = 6 each group). *$P < 0.05$.

collagen, which is known to be only weakly excitable [44]. The high resistance of the fibrous tissue blocks myocardial electrical propagation and may contribute to macro re-entrant circuits and ventricular arrhythmias [45]. To determine whether the injection of a conductive polymeric hydrogel into the scar tissue may reduce its spontaneous cardiac arrhythmias, ambulatory telemetric ECG recordings were obtained four weeks after injection of the test hydrogel. During 72 h of continuous recording, the infarcted animals exhibited consistent PVCs (Fig. 7a), but the PAMB-G hydrogel group had fewer PVCs per hour than did the gelatin hydrogel group ($P < 0.05$, Fig. 7b).

To investigate the susceptibility of infarcted hearts to cardiac arrhythmias, the standard clinical method, PES, was adopted to induce arrhythmias. Four weeks post-hydrogel injection, the rat hearts were subjected to PES to determine the effects of hydrogel injection on PVC induction (Fig. 7c). Upon challenged with PES, arrhythmia susceptibility measured by the inducibility quotient was significantly lower in rats that had been injected with the PAMB-G hydrogel than in those that had been injected with the gelatin hydrogel ($P < 0.05$, Fig. 7d), suggesting a lower probability of arrhythmia in the PAMB-G hydrogel group.

3.8. Electrical impulse conduction velocity across infarct scar region

To evaluate electrical impulse conduction velocity in the left ventricle, hearts of healthy rats (without MI) and of rats that had been injected with the gelatin or PAMB-G hydrogel post-MI were excised at the end of the study (at four weeks) and Langendorff-perfused. A voltage-sensitive dye (di-4-ANEPPS) was perfused to measure the electrical impulse conduction velocity across the normal and infarct scar regions in all groups (Fig. 7e). Fig. 7f reveals that the hearts that were treated with either test hydrogel had a significantly lower electrical impulse conduction velocity than normal hearts ($P < 0.05$). However, the electrical impulse conduction velocity in the PAMB-G-injected hearts significantly exceeded that in the gelatin-injected hearts ($P < 0.05$). These results suggest that PAMB-G hydrogel injection improved electrical impulse propagation across the scar tissue and activated surviving viable contracting regions to provide an electrical bridge across the fibrous scar barrier between functioning myocardia.

3.9. Cardiac function and histological findings

To determine whether the improved electrical impulse propagation translates into functional recovery, cardiac function was evaluated by echocardiography at four weeks post-hydrogel injection (Fig. 8a). The PAMB-G-injected hearts exhibited significantly greater fractional shortening and ejection fraction ($P < 0.05$, Fig. 8b and c) and significantly lower LVIDs and LVIDd ($P < 0.05$, Fig. 8d and e) than the gelatin-injected hearts. In addition, the scars were significantly smaller and scar thickness was significantly greater in the PAMB-G group than in the gelatin group ($P < 0.05$, Fig. 8f and g). The fraction of the myocardium that was viable (red under Masson's trichrome staining) in the total infarcted area at four weeks post-hydrogel injection was significantly greater in the PAMB-G group than in the gelatin group, suggesting higher myocardial tissue survival in the PAMB-G group ($P < 0.05$, Fig. 8g). The presence of viable myocardium was further confirmed via detecting SARC and connexin 43 in the infarcted region using immunofluorescent staining (Fig. S2). Previous studies have demonstrated that collateral blood vessels from the border area can grow into the scar area and thereby support the survival of cardiac cells in an infarcted myocardium [46–48].

Histological findings revealed minimal infiltrating immune cells in the infarcted area (H&E staining, Fig. 8h) and a lack of encapsulation

(Masson's trichrome staining, Fig. 8i) in both studied groups, implying the biocompatibility of both test hydrogels. The gelatin backbone in the PAMB-G hydrogel may be degraded by gelatinase over time; however, the grafted PAMB is non-degradable and may remain intact in extracellular matrices and continue to increase regional conduction.

Many mechanisms are likely to be responsible for the improvement of cardiac function by conductive PAMB-G hydrogel. The improvement in electrical impulse propagation across the scarred tissue as a result of PAMB-G hydrogel permits the timed contraction of viable myocardia that are isolated by the infarct scar and facilitates their synchronous contraction (Figs. 5, 7e and 7f), improving cardiac function. Appropriate electrical stimulation may also promote matrix remodeling, preventing ventricular thinning and dilatation (Fig. 8f and g). In addition, the resulting increase in electrical conduction in the scar may reduce the number of unidirectional exit blockages, reducing the probability of the formation of re-entrant circuits in ventricular arrhythmia [49,50].

4. Conclusions

The above results demonstrate that the as-proposed PAMB-G hydrogel is biocompatible and electrically conductive. This gelatin-based conductive hydrogel can transmit biological current from one heart to excite another heart at a distance. The self-doping ability of PABM-G hydrogel can be used to improve electrical activity in fibrotic tissues and to facilitate the propagation of electrical current across scar regions, providing an electrical bridge between functioning myocardium and islands of intact CMs.

Acknowledgments

The authors would like to thank Dr. Leigh Botly for help with manuscript preparation and editing. This work was supported by a grant from the Canadian Institutes of Health Research (332652 awarded to R.-K. L) and grants from the Ministry of Science and Technology (MOST 107-3017-F-007-002) and the Ministry of Education (MOE 107QR001I5) of Taiwan, ROC.

Appendix A. Supplementary data

Supplementary data to this article can be found online at https://doi.org/10.1016/j.biomaterials.2019.119672.

References

[1] Y. Sun, K.T. Weber, Infarct scar: a dynamic tissue, Cardiovasc. Res. 46 (2000) 250–256.
[2] P. Menasche, A.A. Hagege, J.T. Vilquin, M. Desnos, E. Abergel, B. Pouzet, et al., Autologous skeletal myoblast transplantation for severe postinfarction left ventricular dysfunction, J. Am. Coll. Cardiol. 41 (2003) 1078–1083.
[3] F. Ruschitzka, W.T. Abraham, J.P. Singh, J.J. Bax, J.S. Borer, J. Brugada, et al., Cardiac-resynchronization therapy in heart failure with a narrow QRS complex, N. Engl. J. Med. 369 (2013) 1395–1405.
[4] J.S. Miller, The 2000 nobel prize in Chemistry – a personal accolade, ChemPhysChem 1 (2000) 229–230.
[5] C.E. Schmidt, V.R. Shastri, J.P. Vacanti, R. Langer, Stimulation of neurite outgrowth using an electrically conducting polymer, Proc. Natl. Acad. Sci. U.S.A. 94 (1997) 8948–8953.
[6] J.H. Huang, X.Y. Hu, L. Lu, Z. Ye, Q.Y. Zhang, Z.J. Luo, Electrical regulation of Schwann cells using conductive polypyrrole/chitosan polymers, J. Biomed. Mater. Res. A 93 (2010) 164–174.
[7] B. Guo, J. Qu, X. Zhao, M. Zhang, Degradable conductive self-healing hydrogels based on dextran-graft-tetraaniline and N-carboxyethyl chitosan as injectable carriers for myoblast cell therapy and muscle regeneration, Acta Biomater. 84 (2019) 180–193.
[8] R. Dong, P.X. Ma, B. Guo, Conductive biomaterials for muscle tissue engineering, Biomaterials 229 (2020) 119584.
[9] T.J. Rivers, T.W. Hudson, C.E. Schmidt, Synthesis of a novel, biodegradable electrically conducting polymer for biomedical applications, Adv. Funct. Mater. 12 (2002) 33–37.
[10] Y. Liang, X. Zhao, T. Hu, Y. Han, B. Guo, Mussel-inspired, antibacterial, conductive, antioxidant, injectable composite hydrogel wound dressing to promote the regeneration of infected skin, J. Colloid Interface Sci. 556 (2019) 514–528.
[11] M. Li, J. Chen, M.T. Shi, H.L. Zhang, P.X. Ma, B.L. Guo, Electroactive anti-oxidant polyurethane elastomers with shape memory property as non-adherent wound dressing to enhance wound healing, Chem. Eng. J. 375 (2019) 121999.
[12] Y.B. Wu, L. Wang, B.L. Guo, P.X. Ma, Interwoven aligned conductive nanofiber yarn/hydrogel composite scaffolds for engineered 3D cardiac anisotropy, ACS Nano 11 (2017) 5646–5659.
[13] B. Guo, P.X. Ma, Conducting polymers for tissue engineering, Biomacromolecules 19 (2018) 1764–1782.
[14] J. Zhou, J. Chen, H. Sun, X. Qiu, Y. Mou, Z. Liu, et al., Engineering the heart: evaluation of conductive nanomaterials for improving implant integration and cardiac function, Sci. Rep. 4 (2014) 3733.
[15] J. Park, S. Choi, A.H. Janardhan, S.Y. Lee, S. Raut, J. Soares, Electromechanical cardioplasty using a wrapped elasto-conductive epicardial mesh, Sci. Transl. Med. 8 (2016) 344ra86.
[16] T.H. Qazi, R. Rai, A.R. Boccaccini, Tissue engineering of electrically responsive tissues using polyaniline based polymers: a review, Biomaterials 35 (2014) 9068–9086.
[17] D. Kai, M.P. Prabhakaran, G. Jin, S. Ramakrishna, Polypyrrole-contained electrospun conductive nanofibrous membranes for cardiac tissue engineering, J. Biomed. Mater. Res. A 99 (2011) 376–385.
[18] L. Xu, S.R. Gutbrod, Y. Ma, A. Petrossians, Y. Liu, R.C. Webb, et al., Materials and fractal designs for 3D multifunctional integumentary membranes with capabilities in cardiac electrotherapy, Adv. Mater. 27 (2015) 1731–1737.
[19] Z. Shi, X. Gao, M.W. Ulah, S. Li, Q. Wang, G. Yang, Electroconductive natural polymer-based hydrogels, Biomaterials 111 (2016) 40–54.
[20] S. Gupta, V. Luthra, R. Singh, Electrical transport and EPR investigations: a comparative study for D.C. conduction mechanism in monovalent and multivalent ions doped polyaniline, Bull. Mater. Sci. 35 (2012) 787–794.
[21] S.C. Kim, J. Whitten, J. Kumar, F.F. Bruno, L.A. Samuelson, Self-doped carboxylated polyaniline: effect of hydrogen bonding on the doping of polymers, Macromol. Res. 17 (2009) 631–637.
[22] B.C. Liu, Y. Wang, Y. Miao, X.Y. Xhang, Z.X. Fan, G. Singh, et al., Hydrogen bonds autonomously powered gelatin methacrylate hydrogels with super-elasticity, self-heal and underwater self-adhesion for sutureless skin and stomach surgery and E-skin, Biomaterials 171 (2018) 83–96.
[23] M. Cabuk, M. Yavuz, H.I. Unal, Y. Alan, Synthesis, characterization, and enhanced antibacterial activity of chitosan-based biodegradable conducting graft copolymers, Polym. Compos. 36 (2014) 497–509.
[24] Y. Liu, J. Hu, X. Zhuang, P. Zhang, Y. Wei, X. Wang, et al., Synthesis and characterization of novel biodegradable and electroactive hydrogel based on aniline oligomer and gelatin, Macromol. Biosci. 12 (2012) 241–250.
[25] D.H. Ma, J.Y. Lai, H.Y. Chang, C.C. Tsai, L.K. Yeh, Carbodiimide cross-linked amniotic membranes for cultivation of limbal epithelial cells, Biomaterials 31 (2010) 6647–6658.
[26] J. Wang, D. Zhao, K. Shang, Y.T. Wang, D.D. Ye, A.H. Kang, et al., Ultrasoft gelatin aerogels for oil contaminant removal, J. Mater. Chem. 4 (2016) 9381–9389.
[27] X.Q. He, M.S. Chen, S.H. Li, S.M. Liu, Y. Zhong, H.Y.M. Kinkaid, et al., Co-culture with cardiomyocytes enhanced the myogenic conversion of mesenchymal stromal cells in a dose-dependent manner, Mol. Cell. Biochem. 339 (2010) 89–98.
[28] R.M. Bell, M.M. Mocanu, D.M. Yellon, Retrograde heart perfusion: the Langendorff technique of isolated heart perfusion, J. Mol. Cell. Cardiol. 50 (2011) 940–950.
[29] T. Nguyen, E.E. Salibi, J.L. Rouleau, Postinfarction survival and inducibility of ventricular arrhythmias in the spontaneously hypertensive rat: effects of ramipril and hydralazine, Circulation 98 (1998) 2074–2080.
[30] D. Shen, X. Wang, L. Zhang, X. Zhao, J. Li, K. Cheng, et al., The amelioration of cardiac dysfunction after myocardial infarction by the injection of keratin biomaterials derived from human hair, Biomaterials 32 (2011) 9290–9299.
[31] W. Wang, B. Tan, J. Chen, R. Bao, X. Zhang, S. Liang, et al., An injectable conductive hydrogel encapsulating plasmid DNA-eNOs and ADSCs for treating myocardial infarction, Biomaterials 160 (2018) 69–81.
[32] K.L. Christman, R.J. Lee, Biomaterials for the treatment of myocardial infarction, J. Am. Coll. Cardiol. 48 (2006) 907–913.
[33] N.F. Huang, J. Yu, R. Sievers, S. Li, R.J. Lee, Injectable biopolymers enhance angiogenesis after myocardial infarction, Tissue Eng. 11 (2005) 1860–1866.
[34] J. Wu, F. Zeng, X.P. Huang, J.C. Chung, F. Konecny, R.D. Weisel, et al., Infarct stabilization and cardiac repair with a VEGF-conjugated, injectable hydrogel, Biomaterials 32 (2011) 579–586.
[35] L.M. Monteiro, F. Vasques-Nóvoa, L. Ferreira, O.P. Pinto-do, D.S. Nascimento, Restoring heart function and electrical integrity: closing the circuit, NPJ Regen. Med. 2 (2017) 9.
[36] J. Stejskal, P. Kratochvil, N. Radhakrishman, Polyaniline dispersions 2. UV-vis absorption spectra, Synth. Met. 61 (1993) 225–231.
[37] A.A. Aimetti, A.J. Machen, K.S. Anseth, Poly(ethylene glycol) hydrogels formed by thiol-ene photopolymerization for enzyme-responsive protein delivery, Biomaterials 30 (2009) 6048–6054.
[38] M. Patenaude, S. Campbell, D. Kinio, T. Hoare, Tuning gelation time and morphology of injectable hydrogels using ketone-hydrazide cross-linking, Biomacromolecules 15 (2014) 781–790.
[39] C. Korupalli, W.Y. Pan, C.Y. Yeh, P.M. Chen, F.L. Mi, H.W. Tsai, et al., Single-injecting, bioinspired nanocomposite hydrogel that can recruit host immune cells *in situ* to elicit potent and long-lasting humoral immune responses, Biomaterials 216 (2019) 119268.
[40] K. Tian, J. Bae, S.E. Bakarich, C. Yang, R.D. Gately, G.M. Spinks, et al., 3D printing of transparent and conductive heterogeneous hydrogel-elastomer systems, Adv. Mater. 29 (2017) 1604827.

[41] B. Bhana, R.K. Iyer, W.L.K. Chen, R. Zhao, K.L. Sider, M. Likhitpanichkul, Influence of substrate stiffness on the phenotype of heart cells, Biotechnol. Bioeng. 105 (2010) 1148–1160.
[42] K.D. Clercq, C. Schelfhout, M. Bracke, O.D. Wever, M.V. Bockstal, W. Ceelen, et al., Genipin crosslinked gelatin microspheres as a strategy to prevent postsurgical peritoneal adhesions: *in vitro* and *in vivo* characterization, Biomaterials 96 (2016) 33–46.
[43] A. Navaei, H. Saini, W. Christenson, R.T. Sullivan, R. Ros, M. Nikkhah, Gold nanorod-incorporated gelatin-based conductive hydrogels for engineering cardiac tissue constructs, Acta Biomater. 41 (2016) 133–146.
[44] E.A. Rog-Zielinska, R.A. Norris, P. Kohl, R. Markwald, The living scar-cardiac fibroblasts and the injured heart, Trends Mol. Med. 22 (2016) 99–114.
[45] C.M. Ripplinger, Q. Lou, W. Li, J. Hadley, I.R. Efimov, Panoramic imaging reveals basic mechanisms of induction and termination of ventricular tachycardia in rabbit heart with chronic infarction: implications for low-voltage cardioversion, Heart Rhythm 6 (2009) 87–97.
[46] G. Agnoletti, A. Cargnoni, L. Agnoletti, M. Di Marcello, P. Balzarini, E. Pasini, et al., Experimental ischemic cardiomyopathy: insights into remodeling, physiological adaptation, and humoral response, Ann. Clin. Lab. Sci. 36 (2006) 333–340.
[47] X.J. Song, C.Y. Yang, B. Liu, Q. Wei, M.T. Korkor, J.Y. Liu, et al., Atorvastatin inhibits myocardial cell apoptosis in a rat model with post myocardial infarction heart failure by downregulating ER stress response, Int. J. Med. Sci. 8 (2011) 564–572.
[48] D.G. Wang, F.X. Zhang, W.Z. Shen, M.L. Chen, B. Yang, Y.Z. Zhang, et al., Mesenchymal stem cell injection ameliorates the inducibility of ventricular arrhythmias after myocardial infarction in rats, Int. J. Cardiol. 152 (2011) 314–320.
[49] S. Nattel, D. Dobrev, Electrophysiological and molecular mechanisms of paroxysmal atrial fibrillation, Nat. Rev. Cardiol. 13 (2016) 575–590.
[50] E.J. Ciaccio, J. Coromilas, A.L. Wit, N.S. Peter, H. Garan, Source-sink mismatch causing functional conduction block in re-entrant ventricular tachycardia, JACC (J. Am. Coll. Cardiol.): Clin Electrophysiol 4 (2018) 1–16.